

PAPER • OPEN ACCESS

Yellow emitting Iridium (III) phenyl-benzothiazole complexes with different β -diketone ancillary ligands as dopants in white organic light-emitting diodes

To cite this article: P Ivanov *et al* 2018 *J. Phys.: Conf. Ser.* **992** 012029

View the [article online](#) for updates and enhancements.

You may also like

- [Estimation of exciton reverse transfer for variable spectra and high efficiency in interlayer-based organic light-emitting devices](#)
Shengqiang Liu, Juan Zhao, Jiang Huang et al.
- [Appraisal of Structural, Thermal, and Optical Properties of Novel Bluish-Violet Light-Emitting Cyclometallated Iridium \(III\) \(Cl-H-DPQ\)2Ir\(acac\) Complex for OLED Devices](#)
Neha Khotele, N. Thejo Kalyani, Ramchandra Pode et al.
- [New yellow-emitting phosphorescent cyclometalated iridium\(III\) complex](#)
P Ivanov, R Tomova, P Petrova et al.



ECS
The
Electrochemical
Society
Advancing solid state &
electrochemical science & technology

DISCOVER
how sustainability
intersects with
electrochemistry & solid
state science research

Yellow emitting Iridium (III) phenyl-benzothiazole complexes with different β -diketone ancillary ligands as dopants in white organic light-emitting diodes

P Ivanov, P Petrova and R Tomova¹

Acad. J. Malinowski Institute of Optical Materials and Technologies,
Bulgarian Academy of Sciences, Acad. G. Bonchev Str., Bl. 109, 1113 Sofia, Bulgaria

E-mail: reni@iomt.bas.bg

Abstract. We discuss the influence of the type of β -diketone ancillary ligand in Iridium (III) bis phenyl-benzothiazole complexes ((bt)₂Ir(β -diketone)) on their photophysical and electroluminescent properties when they are used as dopants in white organic light-emitting diodes (WOLED). For this purpose, we investigated four novel yellow cyclometalated complexes: (bt)₂Ir(dbm), (bt)₂Ir(fmtdbm), (bt)₂Ir(tta) and (bt)₂Ir(bsm), where dbm = 1,3-diphenylpropane-1,3-dionate; fmtdbm = 1-(4-fluorophenyl)-3-(4-methoxyphenyl)propane-1,3-dionate; tta = 4,4,4-trifluoro-1-(thiophene-2-yl)butane-1,3-dionate; and bsm = 1-phenyllicosane-1,3-dionate). To obtain white light by mixing emissions of two complementary colors (yellow emitted by the dopant and blue, by another emitter), we chose the following OLED structure: ITO/doped HTL/EIL/ ETL/M, where ITO was a transparent anode of In₂O₃:SnO₂; M, a metallic Al cathode; HTL, 4,4'-Bis(9H-carbazol-9-yl)biphenyl (CBP) involved in a poly(N-vinylcarbazole) (PVK) matrix; EIL, an electroluminescent layer of aluminum(III)bis(2-methyl-8-quinolinato)-4-phenylphenolate (BALq); and ETL, an electron-transporting layer of zinc(II)bis(2-2-hydroxyphenyl)benzothiazole. We found that all complexes are suitable candidates for fabrication of WOLED. The best results were demonstrated by the device doped with 2 wt % of (bt)₂Ir(bsm), which had twice as high luminescence (1100 cd/m²) and one-and-a-half as high current efficiency (5 cd/A) as the device doped with 1.25 wt % of the known (bt)₂Ir(acac), with its 580 cd/m² and 3.4 cd/A at approximately the same CIE (Commission Internationale de L'Eclairage) (x/y) coordinates of the warm white light emitted by the two devices.

1. Introduction

Phosphorescent organic light-emitting diodes offer an intriguing future for the next generation of flat-panel displays and solid-state lighting sources because of their high quantum efficiency in comparison with fluorescent OLEDs [1-3]. Owing to the spin-statistics, the singlet/triplet ratio of the electro-generated excitons is 25/75 %. As it is known, only singlet excitons decay radiatively, which limits the external quantum efficiency to 25 %. This constraint can be removed by using electrophosphorescent complexes of transition metals, as Ir, Pt and Os [4-6]. These complexes demonstrate efficient intersystem crossing due to the metals with d⁶ electronic configurations allowing

¹ To whom any correspondence should be addressed.



radiative relaxation of excited triplet states. Thus, the light emitted by both type of excitons can be collected, and the external quantum efficiency can be raised up to 100 % [7, 8].

Among all complexes of transition metals, the cyclometalated Iridium(III) complexes are the most promising because of their high thermal stability, short triplet state lifetimes, high photoluminescent quantum yields and quasi-octahedral geometry providing opportunities for controlled entry of appropriate ligands. To improve the color purity and the quantum efficiency of Ir complexes, special attention should be paid to synthesizing compounds with new, or modified, main [4] [8-11] or ancillary [5, 6] ligands. Typically, phosphorescent complexes are used as emitting guests in hole-transporting hosts of carbazole derivatives, as CBP (4,4'-Bis(9H-carbazol-9-yl)biphenyl) and PVK [poly(9-vinylcarbazole)] [7, 12-14] or polyfluorenes [15, 16].

The excited triplet state of the guest molecule is formed by direct recombination of an electron and a hole on the guest molecule or by energy transfer from the host followed by recombination on the guest [17-18]. Generally, the dopant concentration is in the range 3 – 10 wt %. At higher dopant concentrations, undesirable side effects appear in the host-guest system, such as concentration quenching and triplet-triplet annihilation [18-19] that decrease significantly the devices' efficiency.

2-Phenylbenzo[d]thiazole (bt) is a general ligand framework for designing Ir(III) complexes; while $(bt)_2Ir(acac)$ has been the most thoroughly investigated yellow emitter among all Ir(III) complexes. Its popularity is due to the fact that, in combination with a blue emitter, it is particularly promising for fabrication of WOLEDs with a simple design based on emission of two complementary colors [20, 21]. Up to now, many $(bt)_2Ir(acac)$ derivatives with adjustable color, high luminescent efficiency and electroluminescent performances have been synthesized and investigated [10, 21, 22].

All this motivated us to launch a study on the Ir(III) (bt) complexes synthesized earlier [23] that contain different β -diketone ancillary ligands as dopants, and that are intended for producing WOLEDs. The photophysical and electroluminescent properties of these complexes are presented below.

2. Experimental

2.1. Synthesis of iridium complexes

The complexes used in this study, namely, Iridium(III) bis[2-phenylbenzothiazolato-N,C^{2'}](acetylacetonate) $(bt)_2Ir(acac)$, Iridium(III) bis[2-phenylbenzothiazolato-N,C^{2'}](1,3-diphenylpropane-1,3-dionate) $(bt)_2Ir(dbm)$, Iridium(III) bis[2-phenylbenzothiazolato-N,C^{2'}](1-(4-fluorophenyl)-3-(4-methoxyphenyl)propane-1,3-dionate) $(bt)_2Ir(fmtdbm)$, Iridium(III) bis[2-phenylbenzothiazolato-N,C^{2'}](4,4,4-trifluoro-1-(thiophen-2-yl)butane-1,3-dionate) $(bt)_2Ir(tta)$, and Iridium(III) bis[2-phenylbenzothiazolato-N,C^{2'}](1-phenylicosane-1,3-dionate) $(bt)_2Ir(bsm)$ (figure 1)

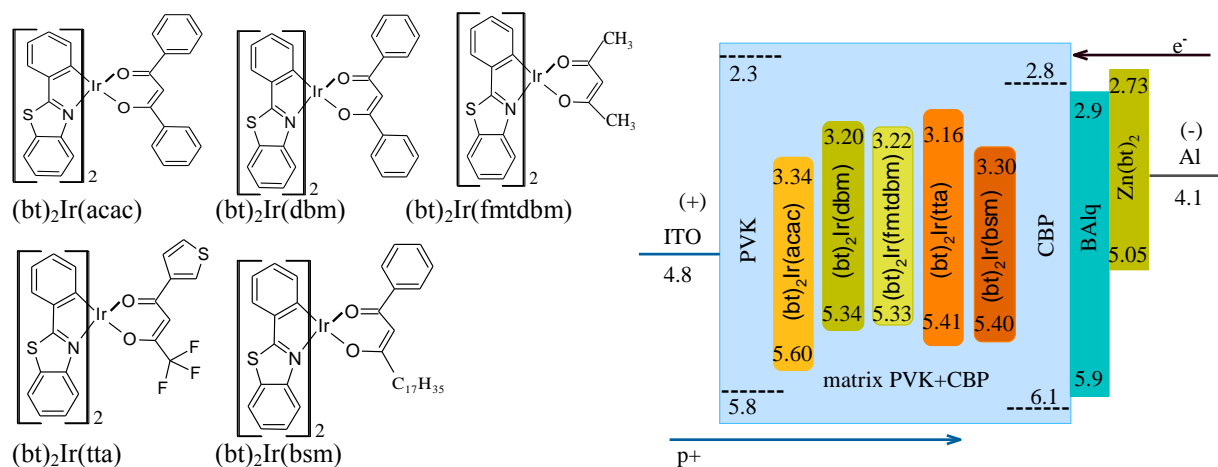


Figure 1. Chemical structure of the Ir(III) complexes used and energy diagram of the OLED investigated. The data for the HOMO/LUMO level are taken from [23].

were synthesized according to a procedure suggested by Nonoyama [24]. The synthesis, characterizations and data for HOMO/LUMO levels, obtained by cyclic voltammetry measurements of cyclometalated Ir(III) complexes were published elsewhere [23].

2.2. Device preparation

We investigated Iridium(III) complexes as dopants in an HTL in a multilayered OLED structure: ITO/doped-HTL/EIL/ETL/M. ITO was a transparent anode of $\text{In}_2\text{O}_3:\text{SnO}_2$, M, a metallic Al cathode; HTL, 4,4'-Bis(9H-carbazol-9-yl)biphenyl (CBP) incorporated in a poly(N-vinylcarbazole) (PVK) matrix; EIL, an electroluminescent layer of aluminum(III)bis(2-methyl-8-quinolinato)-4-phenylphenolate (BAIq); and ETL, an electron-transporting layer of zinc(II) bis(2-(hydroxyphenyl)benzothiazole) ($\text{Zn}(\text{bt})_2$). Devices were prepared with a size of 1 cm^2 on commercial polyethylene terephthalate (PET) substrate coated with ITO ($40\ \Omega/\text{sq}$). The layer of a composite film (30 nm) PVK: CBP_{10%}(relatively to PVK) + Ir(III) complex was deposited by spin-coating at 2000 rpm from 0.75% PVK solution in dichloroethane. All other organic layers: BAIq (40 nm), $\text{Zn}(\text{bt})_2$ (35 nm) and the Al cathode (100 nm) were prepared successively by thermal evaporation in vacuum better than 10^{-4} Pa at rates 2-5 Å/s without disturbing the vacuum. The layers' thicknesses were controlled by a quartz crystal microbalance sensor positioned near the PET/ITO substrate.

2.3. Instruments and measurements

The UV and the fluorescence emission spectra of the Ir complexes investigated were taken in a solution by Thermo Spectronic Unicam 500 and Varian Cary Eclipse spectrophotometers, respectively. The photoluminescence quantum yield (QY) measurements were performed by a Jobin–Yvon–Horiba Fluorolog III apparatus on solution samples using an F-3029 integrating sphere. The luminescent decay times (lifetimes τ) of the complexes in solutions were measured by excitation by a ZWGIGL 300/2 nitrogen laser (wavelength 337.1 nm, pulse duration 2.5 ns, pulse energy 150 μJ). The laser beam was focused on the center of a quartz cuvette with 1 cm optical pathway containing solutions of the complexes (the size of the focused UV laser beam spot was about 200 nm). The timing measurements were performed by a Tektronix TDS 1012B digital oscilloscope and a fast PIN photodiode. The lifetimes were determined by the exponential dependence $I(t) = I(0)\exp(-t/\tau)$, where I is the light intensity at moment (t). The response time of the measuring system was about 10 ns, which determined the accuracy of the lifetime values obtained. The electroluminescence (EL) emission spectra and CIE coordinates of the emitted light were taken by an Ocean Optics HR2000+ spectrometer. The current-voltage (I - V) characteristics were measured using a programmable Labview Keithley 2220-30-1 power supply. The electroluminescence was determined in dc mode and the light output was detected using an S2281-01 Hamamatsu calibrated silicon photodiode. The current efficiency (η_{EL}) used for quantifying the properties of the OLEDs were calculated as

$$\eta_{EL} = EL/I, \text{ cd/A}, \quad (1)$$

where EL is the electroluminescence (cd/m^2) and I is the current density (A/m^2).

3. Result and discussion

3.1. UV-VIS absorption and photoluminescence

The UV-VIS absorption spectra of the Ir(III) complexes and the photoluminescent (PL) spectra of the Ir(III) complexes, CBP and PVK in CH_2Cl_2 , measured under ambient conditions, are shown in figures 2 and 3; their photophysical data are summarized in Table 1. The transitions observed are assigned in accordance with [10]. The absorption spectra shapes of all complexes are very similar, regardless of the varied ancillary ligand. The spectra show a complicated structure due to the overlapping of various bands and are difficult to interpret. The basic absorption bands are observed at about 270 nm and 326 nm. The bands below 300 nm can be attributed to $\pi \rightarrow \pi^*$ transitions in the benzene ring. The absorption at about 326 nm can be referred to LC (ligand-centered) electronic transitions, which lead

to excitations in the bt ligand. The weak bands above 360 nm are assigned to singlet and triplet metal-to-ligand charge transfer bands ($^1\text{MLCT}$, $^3\text{MLCT}$), respectively. The low-intensity bands detectable in the absorption spectrum at 450 nm and 480 nm may be interpreted as resulting from effective spin-orbit coupling (SOC) caused by mixing of the singlet and triplet states. Furthermore, as can be seen in figure 2, the matrices of PVK and CBP emitted blue light with peaks at 367 nm and 385 nm, respectively, providing a good spectral overlapping with the MLCT absorption bands of the Ir(III) complexes ranging from 360 nm to 480 nm, i.e. there is an opportunity for effective Förster or Dexter energy transfer from the host (PVK: CBP) to iridium complex guests. The PL emission spectra of the Ir(III) complexes in non-degassed CH_2Cl_2 without blowing at room temperature obtained under excitation at 330 nm exhibited strong yellow phosphorescence with a maximum emission peak at 558–559 nm and shoulders in 593–601 nm (figure 3).

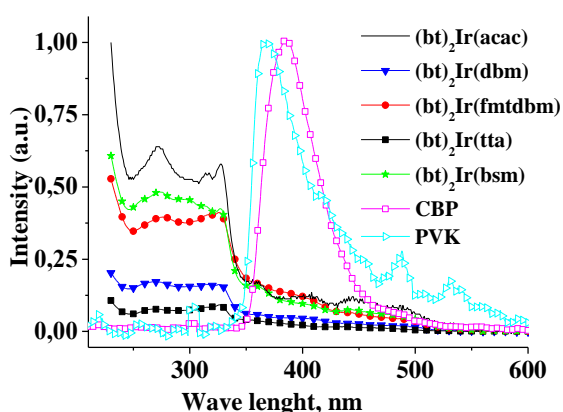


Figure 2. UV-VIS absorption spectra of Ir(III) complexes and PI emission spectra of PVK and CBP in CH_2Cl_2 under ambient conditions.

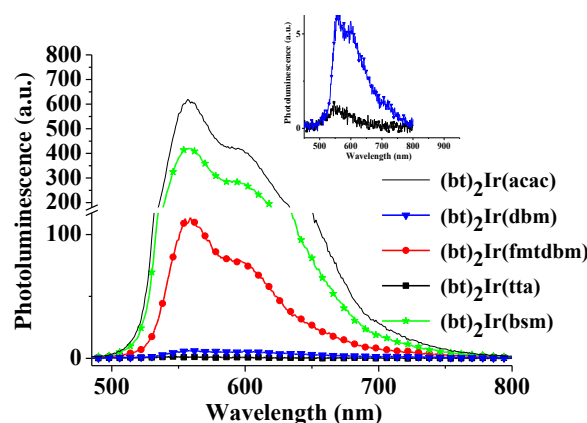


Figure 3. PL emission spectra of the Ir(III) complexes in non-degassed CH_2Cl_2 under ambient conditions.

Only the peak of $(\text{bt})_2\text{Ir}(\text{tta})$ spectrum was blue-shifted by 22 nm in comparison with the other, which was attributed to the presence of electron-withdrawing fluorine atoms on the ancillary ligands. The PI intensities of the complexes were low, especially these of $(\text{bt})_2\text{Ir}(\text{tta})$ and $(\text{bt})_2\text{Ir}(\text{dbm})$ (inset in figure 3), because of the presence of oxygen dissolved in the solution, which is known as a quencher for many fluorophores [25, 26]. It was established that the PI peaks' wavelengths did not shift significantly upon a change of the ancillary ligand in the complexes. The PI data are consistent with the absorption spectral results (figure 2) and indicate that the ancillary ligands: acac, bsm, dbm, tta and fmtdbm, do not seem to change significantly the bandgaps of their complexes and the main bt ligands are the important factor in determining the emission color of the complexes.

As one can see in table 1, the highest QY (0.50) and the longest fluorescence lifetime ($\tau = 200$ ns) were exhibited by $(\text{bt})_2\text{Ir}(\text{acac})$, followed by $(\text{bt})_2\text{Ir}(\text{bsm})$ (QY = 0.20 and $\tau = 210$ ns). Most probably, the presence of aliphatic moieties in the ancillary ligands of $(\text{bt})_2\text{Ir}(\text{acac})$ and $(\text{bt})_2\text{Ir}(\text{bsm})$ imparts some flexibility to the molecules, which reduces the intramolecular quenching and results in the rise observed in the QY and the lifetime. The QYs of $(\text{bt})_2\text{Ir}(\text{fmtdbm})$, $(\text{bt})_2\text{Ir}(\text{dbm})$ and $(\text{bt})_2\text{Ir}(\text{tta})$ were significantly lower and considerably shorter than those of $(\text{bt})_2\text{Ir}(\text{acac})$ and $(\text{bt})_2\text{Ir}(\text{bsm})$. The substitution of acetylacetonate ancillary ligand with different β -diketone lowers the phosphorescent QY, probably because of the appearance of a number of low-energy vibrations enhancing the nonradiative deactivation pathways. That vibronic coupling is a common quenching mechanism for phosphorescent emission.

3.2. Electroluminescence

The EL spectra of the devices undoped and doped with the complexes studied and their electroluminescent characteristics are shown in figures 4a; 5a; 6a; 7a, and figures 4b, 5b; 6b; 7b,

respectively. The EL spectra and their CIE coordinates were taken at 16 V *dc*. For comparison, the EL spectra of devices with HTL and EIL based on only of BALq or Zn(bt)₂ are also presented in figure 5a. As seen, the EL spectrum of the device with BALq has a peak at 496 nm, while that with Zn(bt)₂, at 530 nm. Surprisingly, the EL spectrum shape of the device with evaporated in-series layers of BALq/Zn(bt)₂ was just the same as that of the OLED with EIL of BALq. We believe that, since the HOMO_{Zn(bt)₂} level (5,05 eV) is lower than the HOMO_{BALq} level (5,90 eV) (figure 1), the layer of Zn(bt)₂ cannot retain the holes, which flow unimpeded to the cathode. Therefore, Zn(bt)₂ acts only as an ETL in the BALq/Zn(bt)₂ structure.

Table 1. Photophysical data of the studied complexes in CH₂Cl₂ solution.

| Complex | Absorption λ [nm] (lg ϵ)* | Emission λ_{\max} /shoulder[nm] | Quantum yield (QY) | Lifetime τ [ns] |
|------------------------------|--|--|-----------------------|-------------------------|
| (bt) ₂ Ir(acac) | 272(3.93),315(3.86),327(3.88), 407(3.21), 442(3.19), 489(3.03) | 558/593 | 0.50 | 210 |
| (bt) ₂ Ir(dbm) | 269(4.23),315(4.21),327(4.21), 362(3.75),407(3.64),445(3.45), 492(3.25) | 558/600 | <0.01 | 18 |
| (bt) ₂ Ir(fmtdbm) | 276(4.60),316(4.61),326(4.61), 400(4.08), 492(3.60) | 559/600 | 0.02 | 80 |
| (bt) ₂ Ir(tta) | 269(3.89),315(3.92),327(3.96), 434(3.23) | 546 | <0.01 | 110 |
| (bt) ₂ Ir(bsm) | 273(4.68),298(4.66),314(4.64), 327(4.63), 359(4.19), 400(3.98), 444(3.88), 485(3.75) | 559/601 | 0.20 | 200 |

* ϵ is the molar extinction coefficient (molar absorptivity); The absolute photoluminescence quantum yields (QY) were determined by using rhodamine B as a reference.

The doped devices' EL spectra were basically the sum of the BALq emission (at 496 nm) and those of the Ir complexes at 556 nm for (bt)₂Ir(dbm); 557 nm for (bt)₂Ir(acac) and (bt)₂Ir(fmtdbm); and 558 nm for (bt)₂Ir(bsm). The fact that the EL peaks' positions of these four dopants in OLEDs were almost identical with their PL peaks in solution (figure 3) indicated that EL and PL originate from the same excited state and strongly suggested the absence of any appreciable aggregates from complexes in the solid state. The absence of any emission peaks of PVK and CBP pointed to an effective charge trapping on the Ir(III) complexes and/or an effective energy transfer to the Ir(III) complexes. The only exception were devices doped with (bt)₂Ir(tta), in whose EL spectra the peak of (bt)₂Ir(tta) at 546 nm was missing, but that at 524 nm was present (figure 8a).

As the dopant concentration was raised, the relative intensity of the greenish-blue emission at 496 nm decreased, while that of the yellow one at 556-558 nm grew (figures 4a-8a). Furthermore, the CIE (*x/y*) coordinates of OLEDs were red-shifted from light blue 0,2015/0,3453 for the undoped device to white for different concentrations of different dopants (6 wt % for (bt)₂Ir(dbm) – 0,3368/0,4152; 6 wt % for (bt)₂Ir(tta) – 0,2851/0,4380; 4 wt % for (bt)₂Ir(fmtdbm) – 0,3338/0,4048; 2 wt % for (bt)₂Ir(bsm) – 0,3378/0,4237; 1,25 wt % for (bt)₂Ir(acac) – 0,2981/0,4390); and to different nuances of yellow for devices doped with 10 wt % of: (bt)₂Ir(fmtdbm) – 0,3562/0,4224; (bt)₂Ir(dbm) – 0,3452/0,4407; (bt)₂Ir(bsm) – 0,3810/0,4512; (bt)₂Ir(acac) – 0,4311/0,4522 and (bt)₂Ir(tta) – 0,2581/0,4015. At the same time, the threshold voltage of all devices initially increased at lower dopant concentration and subsequently decreased, without reaching the value of the respective undoped device within the range of tested dopant concentrations. The other characteristics: electroluminescence (*EL*) at

16 V *dc* and current efficiency (η_{El}) at electroluminescence 250 cd/m^2 had just the opposite behavior – initially decreased and then increased with increasing the dopant concentrations (figures 4b-8b).

The best performance was demonstrated by the OLED doped with $(\text{bt})_2\text{Ir}(\text{bsm})$ (figure 4b), whose *El* maximum reached 1600 cd/m^2 and η_{El} , 6.5 cd/A at 8 wt % of dopant, followed by the devices doped with $(\text{bt})_2\text{Ir}(\text{dbm})$ with *El* = 1220 cd/m^2 and η_{El} = 4.72 cd/A at 6 wt %; $(\text{bt})_2\text{Ir}(\text{acac})$ with *El* = 720 cd/m^2 and η_{El} = 4.67 cd/A at 10 wt %; $(\text{bt})_2\text{Ir}(\text{fmtdbm})$ with *El* = 617 cd/m^2 and η_{El} = 4.28 cd/A at 8 wt %; and finally $(\text{bt})_2\text{Ir}(\text{tta})$ with *El* = 667 cd/m^2 and η_{El} = 4.27 cd/A at 8 wt %.

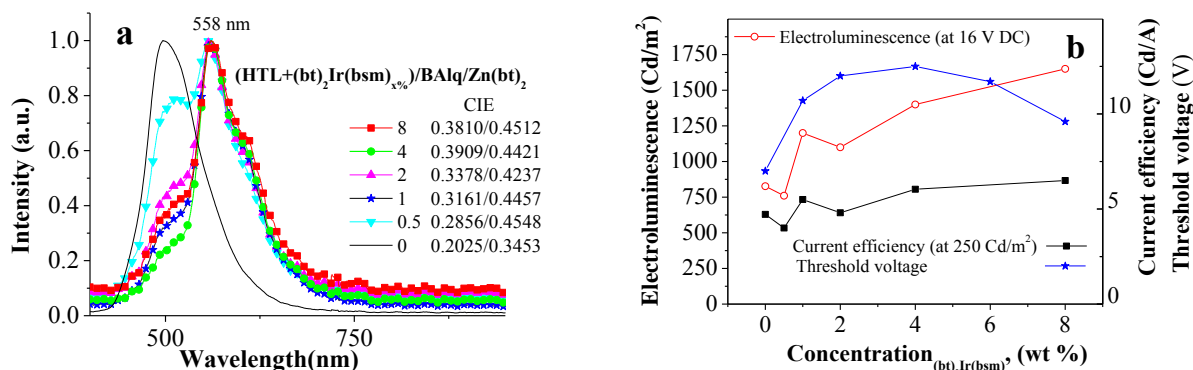


Figure 4. Undoped and doped with $(\text{bt})_2\text{Ir}(\text{bsm})$ devices: **a)** El spectra and CIE coordinates at 16 V DC and **b)** electroluminescence, current efficiency and threshold voltage.

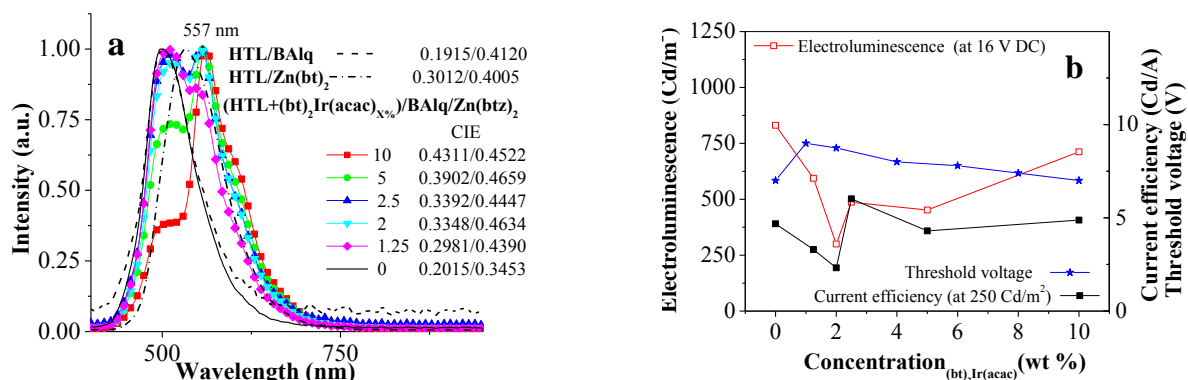


Figure 5. **a)** El spectra and CIE coordinates at 16 V DC for undoped and doped with $(\text{bt})_2\text{Ir}(\text{acac})$ devices and OLED structures: HTL/BAIq and HTL/Zn(bt)₂; **b)** electroluminescence, current efficiency and threshold voltage.

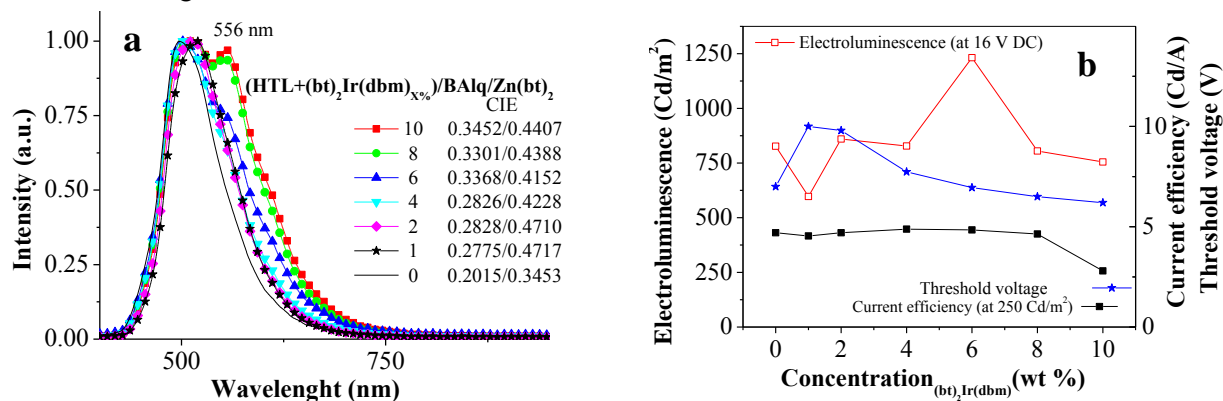


Figure 6. Undoped and doped with $(\text{bt})_2\text{Ir}(\text{dbm})$ devices: **a)** El spectra and CIE coordinates at 16 V DC and **b)** current efficiency and threshold voltage.

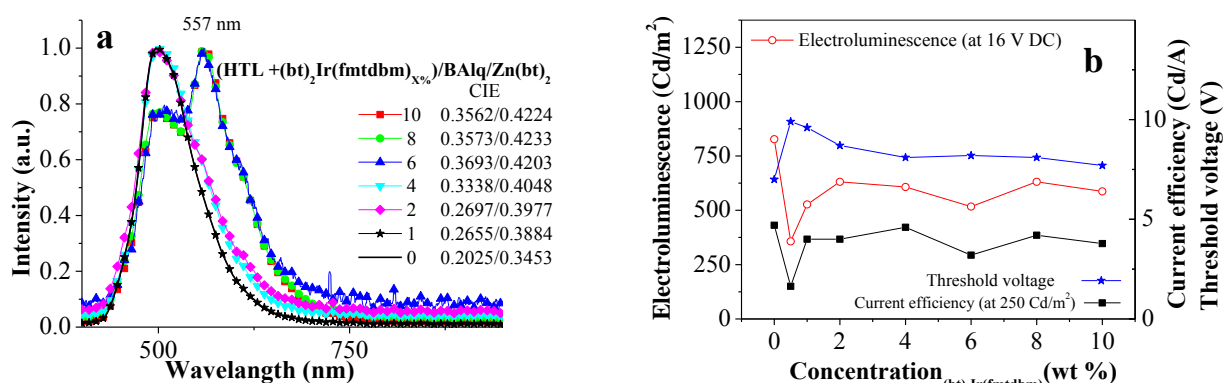


Figure 7. Undoped and doped with (bt)₂Ir(fmtdbm) devices: **a)** El spectra and CIE coordinates at 16 V DC and **b)** electroluminescence, current efficiency and threshold voltage.

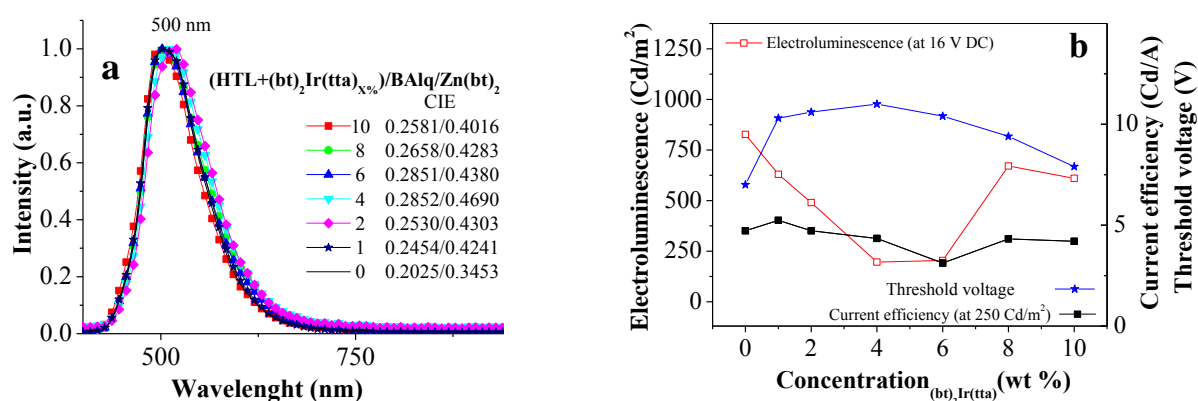


Figure 8. Undoped and doped with (bt)₂Ir(tta) devices: **a)** El spectra and CIE coordinates at 16 V DC and **b)** electroluminescence, current efficiency and threshold voltage.

The decrease of the OLEDs efficiencies as the dopant concentration was increased, on the one hand, and the absence of any PVK and CBP emission in the EL spectra of doped devices, even at low dopant concentrations, on the other, are indicative of charge trapping in the Ir complex, rather than energy transfer, as the dominant mechanism in the OLEDs studied. Since the low dopant concentrations cause mobility limitations associated with the motion of a charge from one dopant site to another, a rise in the devices' threshold voltage was originally observed [6]. Increasing the dopant concentration improves the charge mobility; correspondingly, the current density and the light intensity start increasing and the threshold voltage decreases.

4. Conclusions

The effect was studied of the four β -diketone ancillary ligands (bsm, dbm, tta and fmtdbm) on the photophysical and electroluminescent properties of the iridium phenyl-benzothiazole complexes. All complexes exhibited PL peaks around 560 nm. The change of the ancillary ligand in them did not affect their PL characteristics significantly, thus evidencing that the base bt ligands play a key role in determining the complexes' emission color.

We investigated the possibilities of applying these complexes in OLEDs and found that they are very promising candidates as dopants for producing white OLEDs. The optimal concentration (x) for various different dopants in the OLED structure investigated varied in the range between 1 wt % and 6 wt %. The best performance was demonstrated by the device doped with 2 wt % of (bt)₂Ir(bsm), which had twice as high electroluminescence and one-and-a-half times as high current efficiency in

comparison with the device doped with the already known (bt)₂Ir(acac), at approximately the same CIE (x/y) coordinates of the warm white light emitted by the two devices.

References

- [1] Baldo M, O'Brien D, You Y, Shoustikov A, Sibley S, Thompson M and Forrest S 1998 *Nature* **395** 151-4
- [2] D'Andrade B W and Forrest S R 2004 *Adv. Mater.* **16** 1585- 95
- [3] Wang L, Jiang Y, Luo J, Zhou Y, Zhou J, Wang J, Pei J and Cao Y 2009 *Adv. Mater.* **21** 4854-8
- [4] Choi J, Jung C, Kwon J, Cho H, Lee J, Lee J-Ik, Chu H and Hwang D 2009 *Synth. Met.* **159** 1517-21
- [5] Liu Z, Bian Z, Ming L, Ding F, Shen H, Nie D and Huang C 2008 *Org. Electron.* **9** 171-82
- [6] Hu J, Zhang J, Shih H, Jiang X, Sun P and Cheng C 2008 *J. Organomet. Chem.* **693** 2798-802
- [7] Bauer R, Finkenzeller W, Bogner U, Thompson M and Yersin H 2008 *Org. Electron.* **9** 641-8
- [8] Wang R, Deng L, Zhang T and Li J 2012 *Dalton Trans.* **41** 6833-41
- [9] Seo J, Lee S, Kim Y K and Kim Y S 2008 *Thin Solid Films* **517** 1346-8
- [10] Lamansky S, Djurovich P, Murphy D, Razzaq F, Lee H, Adachi C, Burrows P, Forrest S and Thompson M 2001 *J. Am. Chem. Soc.* **12** 4304-12
- [11] Zhang L, Li L, Shi L and Li W 2009 *Opt. Mater.* **31** 905-11
- [12] Tavasli M, Moore T, Zheng Y, Bryce M, Fox M, Griffiths G, Jankus V, Al-Attar H and Monkman A 2012 *J. Mater. Chem.* **22** 6419- 28
- [13] Kawamura Y, Goushi K, Brooks J, Brown J, Sasabe H and Adachi C 2005 *Appl. Phys. Lett.* **86** 071104
- [14] Adachi C, Baldo M, Forrest S, Lemanski S, Thompson M and Kwong R 2001 *Appl. Phys. Lett.* **78** 1622-4
- [15] Ha S and Noh Y 2013 *Jpn. J. Appl. Phys.* **52** 10MB11
- [16] Miniak H, Teicher M, Scherf U, Trost S, Riedl Th, Lehnhardt M, Rabe T, Kowalsky W and Lochbrunner S 2012 *Phys. Rev. B* **85** 214204
- [17] Baldo M, Lamansky S, Burrows P, Thompson M and Forrest S 1999 *Appl. Phys. Lett.* **75** 4-7
- [18] Baldo M and Forrest S 2000 *Phys. Rev. B* **62** 10958-67
- [19] Baldo M, Adachi C and Forrest S 2000 *Phys. Rev. B* **62** 10967-78
- [20] Liu W and Huang W 2013 *ECS J. Solid State Sci. and Technol.* **2/1** R16-20
- [21] Liu D, Ren H, Deng L and Zhang T 2013 *ACS Appl. Mater. Inter.* **5** 4937-44
- [22] Li M, Zeng H, Meng Y, Sun H, Liu S, Lu Z, Huang Y and Pu X 2011 *Dalton Trans.* **40** 7153-64
- [23] Petrova P, Ivanov P, Marcheva Y and Tomova R 2013 *Bulgarian Chem. Commun.* **45 B** 159-64
- [24] Nonoyama M 1974 *Bull. Chem. Soc. Jpn.* **47** 767-8
- [25] Arik M and Yavuz N 2005 *J. Photochem. Photobiol. A Chem.* **170** 105-11
- [26] Weber G and Lakowicz R 1973 *Chem. Phys. Lett.* **22** 419-23